ORIGINAL ARTICLE

De novo gain-of-function and loss-of-function mutations of *SCN8A* in patients with intellectual disabilities and epilepsy

Maxime G Blanchard,[1] Marjolein H Willemsen,[2] Jaclyn B Walker,[3] Sulayman D Dib-Hajj,[4,5] Stephen G Waxman,[4,5] Marjolijn CJ Jongmans,[2] Tjitske Kleefstra,[2] Bart P van de Warrenburg,[6] Peter Praamstra,[6] Joost Nicolai,[7,8] Helger G Yntema,[2] René JM Bindels,[1] Miriam H Meisler,[3] Erik-Jan Kamsteeg[2]

▶ Additional material is published online only. To view please visit the journal online (http://dx.doi.org/10.1136/jmedgenet-2014-102813).

For numbered affiliations see end of article.

Correspondence to
Dr Erik-Jan Kamsteeg, Department of Human Genetics, Radboud University Medical Center, Nijmegen 6500 HB, The Netherlands; Erik-Jan.Kamsteeg@radboudumc.nl

MHM and EJK share senior coauthorship.

Received 7 October 2014
Revised 1 February 2015
Accepted 5 February 2015
Published Online First 27 February 2015

To cite: Blanchard MG, Willemsen MH, Walker JB, *et al*. *J Med Genet* 2015;**52**:330–337.

ABSTRACT

Background Mutations of *SCN8A* encoding the neuronal voltage-gated sodium channel $Na_V1.6$ are associated with early-infantile epileptic encephalopathy type 13 (EIEE13) and intellectual disability. Using clinical exome sequencing, we have detected three novel de novo *SCN8A* mutations in patients with intellectual disabilities, and variable clinical features including seizures in two patients. To determine the causality of these *SCN8A* mutations in the disease of those three patients, we aimed to study the (dys)function of the mutant sodium channels.

Methods The functional consequences of the three *SCN8A* mutations were assessed using electrophysiological analyses in transfected cells. Genotype–phenotype correlations of these and other cases were related to the functional analyses.

Results The first mutant displayed a 10 mV hyperpolarising shift in voltage dependence of activation (gain of function), the second did not form functional channels (loss of function), while the third mutation was functionally indistinguishable from the wildtype channel.

Conclusions Comparison of the clinical features of these patients with those in the literature suggests that gain-of-function mutations are associated with severe EIEE, while heterozygous loss-of-function mutations cause intellectual disability with or without seizures. These data demonstrate that functional analysis of missense mutations detected by clinical exome sequencing, both inherited and de novo, is valuable for clinical interpretation in the age of massive parallel sequencing.

INTRODUCTION

Exome sequencing has revolutionised the detection of disease-causing mutations, both in research and in diagnostic laboratories. The ease of exome-wide sequencing has led to the discovery of unanticipated associations between gene mutations and disease. However, there is a risk of overinterpreting the role of private mutations in a given gene with disease. Thus, a combination of segregation analysis, metabolic testing and/or functional studies is increasingly important to establish the link between isolated mutations and a patient's disorder.

Nine genes encoding distinct voltage-gated Na^+ channel α subunits $Na_V1.1$–1.9 have been identified and functionally characterised.[1] The gene *SCN8A* encodes the $Na_V1.6$ α subunit, which is abundantly expressed throughout the central nervous system, including high expression in the cerebellum, hippocampus, cortex and olfactory bulb.[2–6] Primary motor neurons as well as cerebellar Purkinje and granule cells have strong expression of $Na_V1.6$, suggesting a role in motor control.[2 3 7] $Na_V1.6$ channels are enriched at the neuronal axon initial segment and nodes of Ranvier, where they promote neuronal excitability by participating in the initiation and propagation of action potentials.[8–12] $Na_V1.6$ channels generate persistent current, hyperpolarised thresholds of activation compared with other Na_V channels, and resurgent current (reviewed in[13]). These biophysical properties make $Na_V1.6$ a critical mediator of neuronal excitability.

Homozygous null mice lacking functional $Na_V1.6$ display severe motor deficits[4 14–16] and impaired learning,[17] while heterozygous null animals display absence epilepsy,[18] disturbed sleep pattern[19] and anxiety.[13 20] Pathological-induced or drug-induced increases in $Na_V1.6$ activity have been associated with susceptibility to epilepsy.[21–23] In humans, an inherited frameshift mutation in *SCN8A* was identified in a child with intellectual disability (ID), ataxia and attention-deficit hyperactivity disorder (ADHD).[24] This frameshift mutation was also present in the patient's mother and maternal aunt, who had ID without ataxia, and in a maternal nephew with isolated ADHD. In 2012, the first de novo *SCN8A* missense mutation was described in a child with severe epileptic encephalopathy.[25] Recently, >30 de novo mutations in *SCN8A* have been identified in patients suffering from early-infantile epileptic encephalopathy type 13 (EIEE13), characterised by early-onset (refractory) epilepsy, features of autism and ID.[26–32] Only three of these mutations have been subjected to functional analysis to determine the consequences for $Na_V1.6$ channel activity.[25 28 32] Two of the tested mutants, p.(Asn1768Asp) and p.(Thr767Ile), induced gain-of-function effects and hyperactivity, suggesting that EIEE13 can be caused by elevated $Na_V1.6$ activity.

Here, using clinical exome sequencing in patients with ID, we identified three novel de novo mutations in *SCN8A*. The patients had ID with additional variable symptoms, including seizures, abnormalities

on brain MRI, spasticity and facial dysmorphisms. We carried out electrophysiological analysis to characterise the effects of the identified mutations on the activity of the mutant $Na_V1.6$ channels. This analysis demonstrated one mutation with gain-of-function and elevated channel activity, one with apparent loss of function and a third with no detectable functional effects. These results are discussed with respect to the individual clinical phenotypes.

METHODS

Patients and clinical exome sequencing

The patients were referred to the Department of Human Genetics of the Radboud University Medical Center (Nijmegen, the Netherlands) for genetic diagnostic evaluation of unexplained ID/developmental delay and/or a movement disorder. Clinical exome sequencing was part of the routine diagnostic procedure. Previous genome-wide chromosomal analyses gave normal results. Patients 1 and 3 were assessed through a family-based exome sequencing ('trio'-exome sequencing) approach.[33 34] Patient 2, who also had ID, was part of a cohort of approximately 100 patients with movement disorders, predominantly ataxia or spastic paraplegia. Exome sequencing was performed essentially as described previously[35] and in online supplementary data.

Cell culture and transfection

Human embryonic kidney cells (HEK293) were grown at 37°C in Dulbecco's modified Eagle's medium (Biowhittaker Europe, Vervier, Belgium) supplemented with 10% (v/v) fetal calf serum (PAA Laboratories, Linz, Austria), non-essential amino acids and 2 mM L-glutamine in a humidified 5% (v/v) CO_2 atmosphere. Cells were seeded in 12-well plates and subsequently transfected with 1.5 µg of $Na_V1.6$ construct and 150 ng enhanced green fluorescent protein using Lipofectamine 2000 (Invitrogen). Three mutations were introduced into the tetrodotoxin (TTX)-resistant derivative of the murine $Na_V1.6$ cDNA clone $Na_V1.6R$ as described previously.[25 28 32] Analysis of human mutations in the context of this TTX-resistant cDNA has facilitated the delineation of biophysical changes produced by human mutations in $Na_v1.6$.[25 28] The three substituted amino acids (D58, N984 and G1451) are conserved between human and mouse $Na_V1.6$ (figure 1). The 6 kb open-reading frame was sequenced to confirm the absence of additional mutations. The day after transfection, cells were seeded on glass coverslips coated with 50 µg/mL of fibronectin (Roche, Mannheim, Germany). Approximately 20 h after transfection, cells were placed in the recording chamber and selected for recording based on intensity of fluorescent reporter.

Electrophysiology

Measurements were carried out at the Department of Physiology (Radboud University Medical Center, the Netherlands) with an EPC9 patch clamp amplifier and Patchmaster software (HEKA electronics, Lambrecht, Germany). The sampling interval was set at 50 µs (20 kHz) and low-pass filtering was set to 5.0 kHz in all

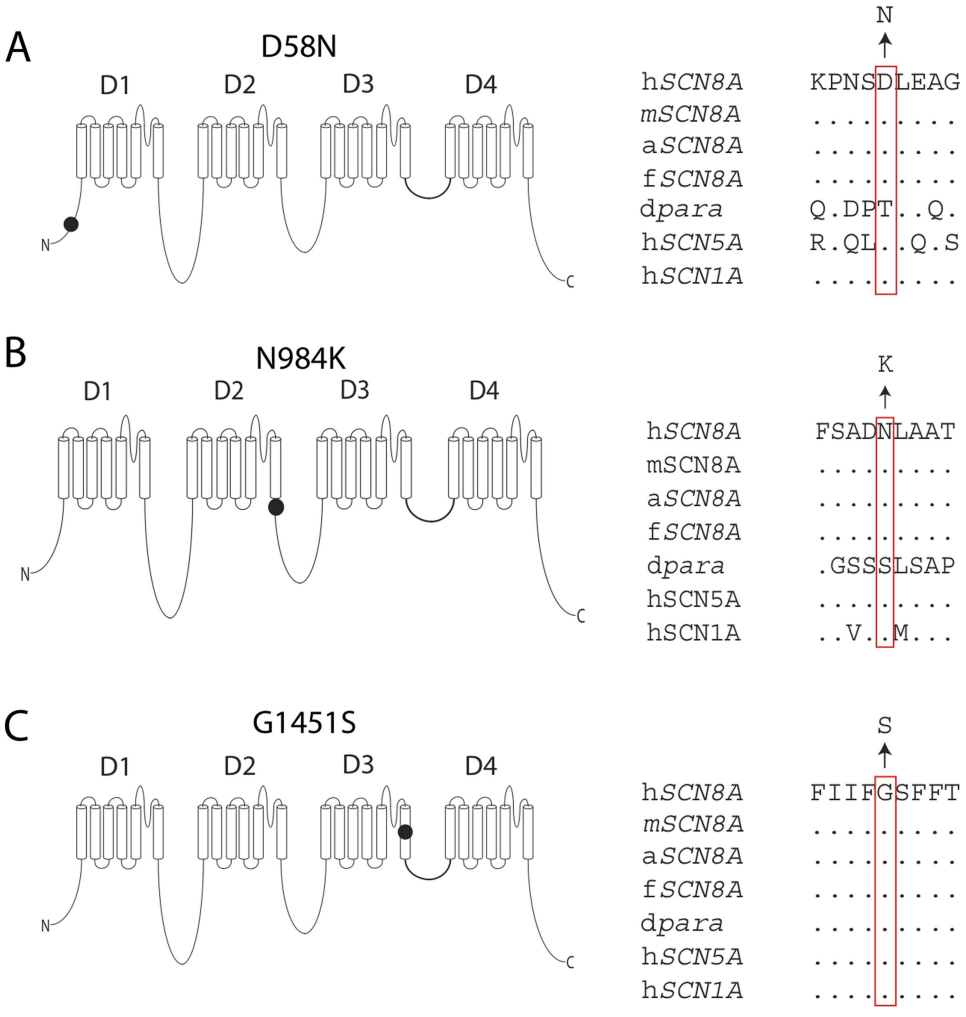

Figure 1 Localisation and evolutionary conservation of three newly identified de novo mutations in *SCN8A* encoding the sodium channel $Na_V1.6$. (A) The D58 residue in the N-terminus. (B) N984 in the intracellular loop close to the sixth transmembrane helix of domain 2 (D2S6). (C) G1451 in the sixth transmembrane helix of domain 3 (DIIIS6), in close proximity to the channel pore. h, *Homo sapiens*; m, *Mus musculus*; a, *Anolis carolinensis* (reptile); f, *Takifugu rubripes* (fish); dpara, *Drosophila melanogaster* 'paralytic' (alternative name Na_V1). Amino acids are indicated by the single-letter code and dots represent identity to the human amino acid. Multiple sequence alignment was carried out using ClustalW V.2.0.12.[48]

experiments. Pipettes were pulled from thin-wall borosilicate glass and had resistances between 0.9 and 1.5 MΩ when filled with the pipette solution. Series resistance compensation was set to 85–95% in all experiments. The leak currents were subtracted using a P/6 procedure from a holding potential of −120 mV.

Currents were activated by 40 ms voltage pulses ranging from −70 to +20 mV (in 10 mV increments) from a holding potential of −120 mV at a sweep frequency of 0.2 Hz. Current–voltage curves were converted to conductance–voltage curve, normalised and individually fitted with a Boltzmann equation (see below). Steady-state inactivation was studied by holding cells at conditioning voltage ranging from −120 to −20 mV (in 10 mV increments) for 500 ms and tested with a 40 ms depolarising pulse to −10 mV. The current elicited after the conditioning voltage period was normalised to the current amplitude obtained from a holding voltage of −120 mV obtained before the conditioning period.

The extracellular solution contained (in mM): 132 NaCl, 4.2 KCl, 1 $CaCl_2$, 1 $MgCl_2$, 10 hydroxyethyl piperazineethanesulfonic acid (HEPES), 25 glucose and pH adjusted to 7.4 with NaOH. The pipette solution contained (in mM): 140 CsF, 10 NaCl, 1 ethylene glycol tetraacetic acid, 10 HEPES and pH adjusted to 7.3 using CsOH. After break-in, a 5 min waiting period permitted equilibration between the pipette solution and the cytoplasm of the cell. Current density was calculated by dividing the current (in pA) by the cell capacitance (in pF).

Statistical analysis and fitting of electrophysiological data

Current–voltage curves were converted to conductance and fitted using the following Boltzmann equation: $g(V)=g_{max}/(1+\exp((V-V_{0.5})/k))$, where g is the conductance, g_{max} is the maximal conductance, V is the voltage, $V_{0.5}$ is the voltage of half-maximal activation and k is the slope factor. Steady-state inactivation curves were fitted with an analogous equation. Data are shown as mean±SEM. The comparisons between mean of the fit parameters and amplitudes were performed using one-way analysis of variance followed by Tukey post hoc test.

Western blotting

To assess protein stability, mutant cDNAs were transfected into HEK293 cells, which lack endogenous sodium channel protein. After culture for 24 h at 37°C, transfected cells were harvested and lysed in radioimmunoprecipitation assay buffer. Aliquots containing 30 µg of protein were incubated with Laemmli sample buffer for 20 min at 37°C, electrophoresed through 4–15% acrylamide gradient gels (Criterion) and immunostained with rabbit polyclonal anti-Nav1.6 (Alomone ASC-009, 1:100). As an internal control, α-tubulin was immunostained with a 1:1000 dilution of monoclonal antibody CLT9002 (Cedarlane Labs, Burlington, Canada).

RESULTS

Clinical phenotypes

In total, 500 patients with ID and 100 patients with a movement disorder were subjected to exome sequencing. Three patients carried mutations of *SCN8A*. One of them was included in the movement disorders group also, despite having an ID, because of his pronounced movement disorder. The clinical features of these patients are summarised in table 1 and in online supplementary data. Patients 1 and 2 experienced seizures and peripheral nervous system disabilities, but these were not present in patient 3.

Mutation detection

In patient 1, a single de novo mutation was revealed after trio-exome sequencing, *SCN8A* (c.2952C>G; p.(Asn984Lys)). This mutation alters an evolutionarily conserved amino acid adjacent to the transmembrane segment of the voltage-gated

Table 1 Clinical features of three patients with de novo mutations in *SCN8A*

Patient	1	2	3
Sex and age	Female, 7 years	Male, 33 years	Male, 33 years
OFC (centile)	51.5 cm (>P50)	55.2 cm (P5–P10)	55,8 cm (P10)
Seizures	Frequent, intractable seizures with an onset at the age of 6 weeks	First seizures at age 18 months, including absences and tonic–clonic seizures	None
DD/ID	Severe DD since birth Not able to sit independently No speech	Moderate to severe DD Walking at age 6 years First words at age 6 years Developmental level at adult age comparable to a 4–5 years old	DD since birth Walking after 18 months Relatively normal speech, but cannot write or read Adult IQ of 55
Neurological symptoms	Neonatal hypertonia Severe dysregulation of muscle tone Neurogenic bladder due to tethered cord	Nystagmus Jerky pursuit Spastic tetraplegia	None
Brain MRI	Progressive cerebral atrophy	Cerebellar atrophy	Cerebral atrophy
Dysmorphisms	Tapering fingers Mild facial dysmorphisms, including synophrys, broad nasal tip and upslanted palpebral fissures	None	Ptosis, asymmetric skull, broad forehead, high palate with narrow uvula, small jaw Clinodactyly second fingers Pectus excavatum
Miscellaneous (non)-neurological	Precocious puberty (6 years) Convex scoliosis Severe feeding difficulties Unexplained spontaneous fractures	Decline in motor, and to a lesser extent in cognitive functioning since the age of 29 years Recurrent falls Swallowing difficulties	Inguinal and umbilical hernia Behaviour problems Mild hypothyroidism
Mutations (de novo)	*SCN8A:* c.2952C>G p.(Asn984Lys) near D2S6	*SCN8A*: c.4351G>A p.(Gly1451Ser) in D3S6	SCN8A: c.172G>A p.(Asp58Asn) in Nterm RING1: c.284G>A; p.(Arg95Gln)

Reference sequences SCN8A: NM_014191.2 and RING1: NM_002931.3. Mutation nomenclature is according to the Human Genome Variation Society guidelines.
DD, developmental delay; ID, intellectual disability; OCF, occipitofrontal circumference.

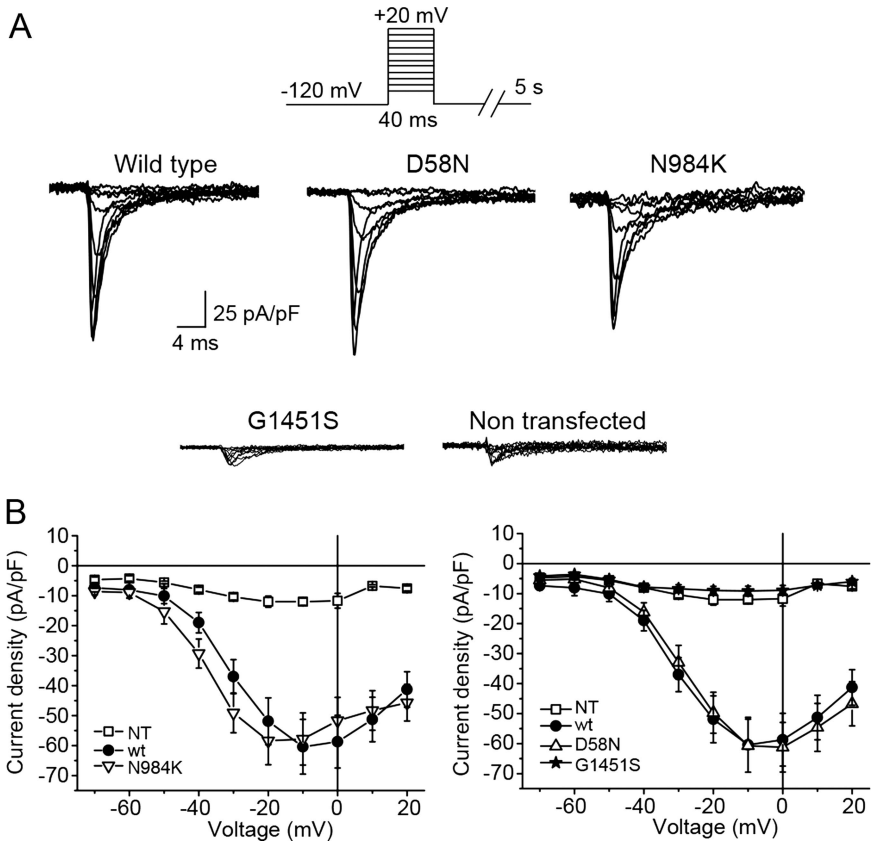

Figure 2 Voltage-evoked currents of mutant proteins in transfected HEK293 cells. (A) Wild type (wt), D58N and N984K gave rise to substantial voltage-evoked currents while the G1451S expressing cells demonstrated current densities similar to non-transfected cells. (B) Average current–voltage curve for non-transfected cells (squares), wt (full circles), D58N (upward triangles), N984K (downward triangles) and G1451S (stars). N=3 for non-transfected cells, and N≥10 for all other conditions.

sodium channel Nav1.6 (N984K; figure 1). Singleton sequencing of patient 2 and analysis for mutations in a movement disorder gene panel (including genes for ataxia, spastic paraplegia and dystonia) did not identify pathogenic variants. After inspection of the full exome data, an *SCN8A* mutation was identified as a candidate (c.4351G>A; p.(Gly1451Ser)). The mutated residue is located in a conserved residue of transmembrane segment D3S6 of Nav1.6 (G1451S; figure 1). Sanger sequencing of parental DNA revealed that this mutation had also occurred de novo. In patient 3, two de novo mutations were identified by trio-exome sequencing, *SCN8A* (c.172G>A; p.(Asp58Asn)) and *RING 1* (c.284G>A; p.(Arg95Gln)). This *SCN8A* mutation alters a residue in the cytoplasmic N-terminus (D58N; figure 1). No likely causative homozygous or compound heterozygous mutations were detected in the exome data of these three patients. Hemizygous mutations were also excluded for patients 2 and 3.

Electrophysiological characterisation of $Na_V1.6$ α subunit mutants

HEK293 cells were transfected with wildtype (wt) or mutated *SCN8A* cDNA encoding the $Na_V1.6$ α subunit and subjected to whole-cell patch clamp measurements essentially as described previously.[36] Cells expressing wt $Na_V1.6$, N984K or D58N demonstrated substantial voltage-evoked currents (figure 2A). Although current amplitudes did not reach their maximal value at the same test voltage, the average maximal inward currents observed for the wt channel and for the D58N and N984K mutants were not statistically different from each other (figure 2B). Current densities in cells expressing the G1451S mutant were ~10-fold smaller than wt transfected cells and were comparable to non-transfected cells (figure 2A). To determine whether the loss of activity of the G1451S was a consequence of protein instability, as recently reported for the R223G mutation,[32] we carried out western blotting. The G1451S mutant proteins were detected in similar levels as wt $Na_V1.6$ in transfected cells (see online supplementary figure S3).

Wt and D58N mutant channels generated currents with similar voltage of half-maximal activation ($V_{0.5}$, figure 3B, see 'Methods' section). Strikingly, the N984K mutant had a 10 mV hyperpolarising shift in $V_{0.5}$ in comparison with wt (figure 3B). The slope factor k of the Boltzmann fit was not different between conditions ($p>0.05$, $n\geq10$). Cells were subjected to a steady-state inactivation protocol in order to study fast inactivation (figure 3C and see 'Methods' section). Currents from cells expressing wt, N984K and D58N demonstrated no statistically significant differences in voltage dependence of steady-state inactivation or slope (figure 3D).

DISCUSSION

We report three novel de novo missense mutations in *SCN8A* identified by clinical exome sequencing in patients with ID and variable clinical features. The degree of developmental delay varied from profound ID in patient 1 to moderate ID in patients 2 and 3. Patients 1 and 2 also presented with epilepsy and a movement disorder (including hypertonia, spasticity and ataxia), whereas patient 3 had no such signs. Comparison of the electrophysiological properties of the mutant channels revealed distinct effects.

Patient 1 is most severely affected clinically, with a diagnosis of EIEE that included onset of intractable seizures at 6 weeks of age, feeding by gastric tube and lack of speech. The N984K mutation of *SCN8A* in this patient resulted in a hyperpolarising shift of ~10 mV in the voltage dependence of activation (figures 2 and 3), which predicts premature channel opening and hyperactivity of neurons. A similar hyperpolarising shift in voltage

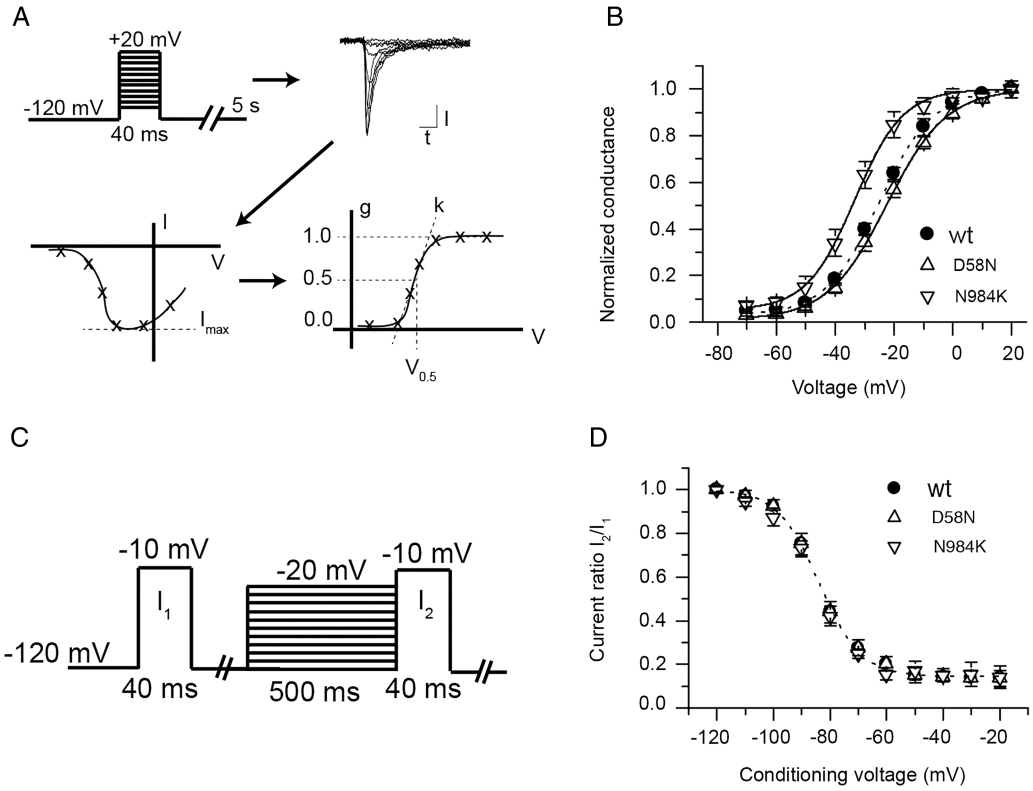

Figure 3 Voltage dependence of activation and steady-state inactivation of mutant proteins in transfected HEK293 cells. (A) Individual current–voltage (I–V) curves were converted to normalised conductance–voltage (g-V) curves and fitted with a Boltzmann equation yielding the voltage of half-maximal activation ($V_{0.5}$) and slope factor (k). (B) Average normalised conductances of wild type (wt), D58N and N984K as a function of voltage. Lines represent Boltzmann fit to the average conductance voltage curve. The N984K mutant $V_{0.5}$ is significantly shifted towards hyperpolarised voltages values ($p<0.05$, $n=10$). $N\geq10$ for each conditions. (C) The protocol used to study steady-state inactivation is shown. The fraction of non-inactivated channels after a 500 ms conditioning period is indicated as the ratio of the current after the conditioning period (I_2) to the current obtained before conditioning (I_1). (D) The average current ratio (I_2/I_1) for wt, D58N and N984K as a function of the conditioning voltage. The dotted line represents a modified Boltzmann fit to the average wt steady-state inactivation curve. Fit to D58N and N984 is not shown for the purpose of clarity. There is no difference in voltage of half-maximal inactivation between wt and mutants ($p>0.05$, $n\geq8$).

dependence of activation of *SCN8A* was recently reported in a severely affected child with the de novo mutation T767I in transmembrane segment D2S1, seizure onset at 2 weeks of age, profound developmental delay and feeding by gastric tube.[28] These two cases, together with the original N1768D mutation,[25] demonstrate clearly that gain-of-function mutations of *SCN8A* that cause elevated channel activity result in severe EIEE.

In patient 2, the G1451S mutation causes apparent loss of channel activity in the HEK cell assay. G1451 is located in a residue of domain 3 that has been suggested to regulate bending of the pore-lining S6 segment during the opening of the channel pore[37] and would be expected to alter channel activity. Patient 2 had later seizure onset, at 18 months of age, and severe developmental delay, but could walk and speak at 6 years of age. In a similar case, the partial loss-of-function mutation R223G was described in a patient with seizure onset at 6 months and profound developmental impairment.[32] Both of these missense mutations generate full-length protein with reduced channel activity and have a severe clinical phenotype including early-onset seizures. Both patients are more severely affected than the family with an SCN8A protein truncation mutation, which resulted in ID without seizures.[24] Two protein truncation mutations have been described in the ESP6500 dataset, but one is an indel of one C nucleotide in a run of four Cs, and the second is a singleton; neither has been confirmed by Sanger sequencing and both must be considered unconfirmed. In three other patients with ID without seizures, loss of *SCN8A* protein due to contiguous gene deletion has been described; at least two were de novo deletions (http://decipher.sanger.ac.uk). The difference between the protein truncation or deletion patients, and the missense patients, suggests that there may be a dominant effect of the full-length inactive proteins with the G1451S and R223G mutations. The mutant proteins could result in sequestration of interacting proteins such as β subunits, which is required for neurite outgrowth and high-frequency neuronal firing of $Na_V1.6$ expressing neurons.[38] Alternatively, there may be gain-of-function features of these proteins that were not detected in the heterologous HEK293 cell assay. Such an observation was made with a mutation of $Na_V1.1$, with apparent loss of function in cultured non-neuronal cells, which was partially rescued in primary cultures of mouse embryo neocortical neurons and exhibited a gain-of-function effect.[39] The subcellular localisation of the G1451S mutant of $Na_V1.6$ has not yet been established, and it will be important to examine this mutant in a neuronal cell assay.

The third patient carried the de novo mutation D58N located in the cytoplasmic N-terminal domain of the protein. Electrophysiological analysis revealed full activity of this mutant channel in HEK cells, with no change in biophysical properties. The N-terminal domain of Nav1.6 is likely to function in protein trafficking rather than channel activity. The mutation

Table 2 Functional analysis of *SCN8A* mutations identified in heterozygous state in patients with intellectual disability (ID) with or without epileptic encephalopathy (EE)

Protein change	ID	EE	Cell assay	Effect on function	Ref.	Channel domain
N1768D	+	+	Neuronal	GOF, increased persistent current	[25]	In D4S6
T1716I	+	+	Neuronal	GOF, hyperpolarizing shift in activation voltage	[28]	In D2S1
N984K	+	+	HEK	GOF, hyperpolarizing shift in activation voltage	This article	Near D2S6
G1451S	+	+	HEK	LOF at 37°C	This article	in D3S6
R223G	+	+	HEK	Partial LOF; thermolabile. Protein is unstable at 37°C, active at 30°C	[32]	In D1S4
P1719Rfs*6	+	–	None	LOF, protein truncation	[24]	In D4S5-S6
D58N	+	–	HEK	Wildtype activity; may be non-pathogenic in view of additional de novo mutation	This article	In N-term

Missense mutations were introduced into the mouse $Na_V1.6$ cDNA and cells were transfected for electrophysiological assays. Only the deduced protein changes (one-letter code) are provided.
GOF, gain of function; LOF, loss of function.

S21P in the N-terminus of mouse Nav1.6 results in protein retention in the endoplasmic reticulum.[40] A binding site for the microtubule-associated protein MAP1B has been mapped between residues 77 and 88 of Nav1.6.[41] The activity of the D58N mutant channel in HEK cells demonstrates successful transport to the cell surface, suggesting that this mutation is not pathogenic. However, it is possible that localisation of the D58N channel to the axon initial segment or node of Ranvier in neurons could be impaired. Nevertheless, with the apparent normal function of the D58N mutants in HEK cells, it is also possible that ID in patient 3 might be caused by the second de novo mutation in the *RING1* gene encoding a E3 ubiquitin ligase. Mutations in *RING1* have not been previously associated with ID. The future detection of similar *SCN8A* or *RING1* mutations may resolve this issue.

Despite the fact that only six *SCN8A* mutations have been tested functionally, preliminary correlations between mutation type and disease severity are emerging (table 2). First, the de novo *SCN8A* mutations in patients with EIEE13, the most severe form of *SCN8A*-related disease, are missense mutations rather than protein truncation mutations.[13] Second, three of these missense mutations clearly result in channel hyperactivity, leading to both seizures and ID. Third, complete loss of function due to protein truncation or gene deletion is associated with isolated ID without seizures[24] (http://decipher.sanger.ac.uk). In the heterologous test systems used for analysis, two missense mutations associated with ID and epilepsy, G1451S and R223G, exhibit (partial) loss-of-function rather than hyperactivity; these merit additional study to detect possible gain-of-function features.

The data for *SCN8A* are in striking contrast with Dravet syndrome, or EIEE6, which is caused by mutations of the sodium channel *SCN1A*. In Dravet, 50% of the >800 de novo mutations in sodium channel *SCN1A* are protein truncation mutations with clear loss of function, and these result in both seizures and ID.[42–44] The milder generalised epilepsy with febrile seizures plus phenotype is associated with missense mutations of *SCN1A*. The difference in the consequences of loss of function may reflect their different roles in inhibitory and excitatory neurons since $Na_V1.6$ (encoded by *SCN8A*) is the major sodium channel in excitatory neurons while $Na_V1.1$ (encoded by *SCN1A*) appears to have a critical role in inhibitory neurons.[45–47]

In summary, we have identified and characterised three novel de novo mutations of *SCN8A*. Electrophysiological studies indicate that one mutation leads to a gain of function (N984K), the second causes apparent loss of function (G1451S) and the third has normal channel activity and may be non-pathogenic (D58N). These data strengthen previous findings linking gain-of-function mutations of *SCN8A* with EIEE and demonstrate the importance of functional testing in establishing the pathogenicity of de novo mutations. Functional characterisation of additional *SCN8A* mutations will provide a more comprehensive understanding of the specific phenotypes associated with gain-of-function and loss-of-function mutations.

Author affiliations
[1]Department of Physiology, Radboud Institute for Molecular Life Sciences, Radboud University Medical Center, Nijmegen, The Netherlands
[2]Department of Human Genetics, Radboud University Medical Center, Nijmegen, The Netherlands
[3]Department of Human Genetics, University of Michigan, Ann Arbor, Michigan, USA
[4]The Center for Neuroscience & Regeneration Research, Yale School of Medicine, New Haven, Connecticut, USA
[5]The Rehabilitation Research Center, VA Connecticut Healthcare System, West Haven, Connecticut, USA
[6]Department of Neurology, Donders Institute for Brain, Cognition and Behavior, Radboud University Medical Center, Nijmegen, The Netherlands
[7]Department of Neurology, Maastricht University Medical Center, Maastricht, The Netherlands
[8]Epilepsy Center Kempenhaeghe, Heeze, The Netherlands

Acknowledgements We thank Janelle O'Brien and Jacy Wagnon for helpful discussions and assistance.

Contributors MGB has contributed to the acquisition, analysis and interpretation of data, and drafting of the manuscript. MHW, JBW, BPvdW, PP, MCJ and JN contributed to data acquisition, interpretation and revising the manuscript for intellectual content. SD-H, SGW, TK, HGY and RJMB contributed to data interpretation and revising the manuscript for intellectual content. MHM and E-JK are accountable for design of the work, interpretation of data and revision for intellectual content. All coauthors have approved the final version of the manuscript. No other persons contributed in a way that they are entitled to be coauthors.

Funding Supported by the National Institutes of Health (R01 NS34509 to MHM). SDH and SGW were supported by grants from the Rehabilitation Research Service, the Veterans Administration, USA.

Competing interests None.

Patient consent Obtained.

Ethics approval Ethics committee of the Radboud University Medical Center.

Provenance and peer review Not commissioned; externally peer reviewed.

Data sharing statement Except for the raw data, no additional data are available. Raw data may be made available if it does not infringe patients rights.

REFERENCES

1 Catterall WA, Goldin AL, Waxman SG. International Union of Pharmacology. XLVII. Nomenclature and structure-function relationships of voltage-gated sodium channels. *Pharmacol Rev* 2005;57:397–409.
2 Schaller KL, Krzemien DM, Yarowsky PJ, Krueger BK, Caldwell JH. A novel, abundant sodium channel expressed in neurons and glia. *J Neurosci* 1995; 15(5 Pt 1):3231–42.
3 Schaller KL, Caldwell JH. Developmental and regional expression of sodium channel isoform NaCh6 in the rat central nervous system. *J Comp Neurol* 2000;420:84–97.
4 Burgess DL, Kohrman DC, Galt J, Plummer NW, Jones JM, Spear B, Meisler MH. Mutation of a new sodium channel gene, Scn8a, in the mouse mutant 'motor endplate disease'. *Nat Genet* 1995;10:461–5.
5 Hu W, Tian C, Li T, Yang M, Hou H, Shu Y. Distinct contributions of Na(v)1.6 and Na(v)1.2 in action potential initiation and backpropagation. *Nat Neurosci* 2009;12:996–1002.
6 Klein JP, Khera DS, Nersesyan H, Kimchi EY, Waxman SG, Blumenfeld H. Dysregulation of sodium channel expression in cortical neurons in a rodent model of absence epilepsy. *Brain Res* 2004;1000:102–9.
7 Schaller KL, Caldwell JH. Expression and distribution of voltage-gated sodium channels in the cerebellum. *Cerebellum* 2003;2:2–9.
8 Gasser A, Ho TS, Cheng X, Chang KJ, Waxman SG, Rasband MN, Dib-Hajj SD. An ankyrinG-binding motif is necessary and sufficient for targeting Nav1.6 sodium channels to axon initial segments and nodes of Ranvier. *J Neurosci* 2012;32:7232–43.
9 Osorio N, Alcaraz G, Padilla F, Couraud F, Delmas P, Crest M. Differential targeting and functional specialization of sodium channels in cultured cerebellar granule cells. *J Physiol* 2005;569(Pt 3):801–16.
10 Van Wart A, Trimmer JS, Matthews G. Polarized distribution of ion channels within microdomains of the axon initial segment. *J Comp Neurol* 2007;500:339–52.
11 Duflocq A, Le Bras B, Bullier E, Couraud F, Davenne M. Nav1.1 is predominantly expressed in nodes of Ranvier and axon initial segments. *Mol Cell Neurosci* 2008;39:180–92.
12 Osorio N, Cathala L, Meisler MH, Crest M, Magistretti J, Delmas P. Persistent Nav1.6 current at axon initial segments tunes spike timing of cerebellar granule cells. *J Physiol* 2010;588(Pt 4):651–70.
13 O'Brien JE, Meisler MH. Sodium channel SCN8A (Nav1.6): properties and de novo mutations in epileptic encephalopathy and intellectual disability. *Front Genet* 2013;4:213.
14 Kohrman DC, Plummer NW, Schuster T, Jones JM, Jang W, Burgess DL, Galt J, Spear BT, Meisler MH. Insertional mutation of the motor endplate disease (med) locus on mouse chromosome 15. *Genomics* 1995;26:171–7.
15 Levin SI, Khaliq ZM, Aman TK, Grieco TM, Kearney JA, Raman IM, Meisler MH. Impaired motor function in mice with cell-specific knockout of sodium channel Scn8a (NaV1.6) in cerebellar purkinje neurons and granule cells. *J Neurophysiol* 2006;96:785–93.
16 Hamann M, Meisler MH, Richter A. Motor disturbances in mice with deficiency of the sodium channel gene Scn8a show features of human dystonia. *Exp Neurol* 2003;184:830–8.
17 Woodruff-Pak DS, Green JT, Levin SI, Meisler MH. Inactivation of sodium channel Scn8A (Na-sub(v)1.6) in Purkinje neurons impairs learning in Morris water maze and delay but not trace eyeblink classical conditioning. *Behav Neurosci* 2006;120:229–40.
18 Papale LA, Beyer B, Jones JM, Sharkey LM, Tufik S, Epstein M, Letts VA, Meisler MH, Frankel WN, Escayg A. Heterozygous mutations of the voltage-gated sodium channel SCN8A are associated with spike-wave discharges and absence epilepsy in mice. *Hum Mol Genet* 2009;18:1633–41.
19 Papale LA, Paul KN, Sawyer NT, Manns JR, Tufik S, Escayg A. Dysfunction of the Scn8a voltage-gated sodium channel alters sleep architecture, reduces diurnal corticosterone levels, and enhances spatial memory. *J Biol Chem* 2010;285:16553–61.
20 McKinney BC, Chow CY, Meisler MH, Murphy GG. Exaggerated emotional behavior in mice heterozygous null for the sodium channel Scn8a (Nav1.6). *Genes Brain Behav* 2008;7:629–38.
21 Sun W, Wagnon JL, Mahaffey CL, Briese M, Ule J, Frankel WN. Aberrant sodium channel activity in the complex seizure disorder of Celf4 mutant mice. *J Physiol* 2013;591(Pt 1):241–55.
22 Hargus NJ, Nigam A, Bertram EH III, Patel MK. Evidence for a role of Nav1.6 in facilitating increases in neuronal hyperexcitability during epileptogenesis. *J Neurophysiol* 2013;110:1144–57.
23 Chen Z, Chen S, Chen L, Zhou J, Dai Q, Yang L, Li X, Zhou L. Long-term increasing co-localization of SCN8A and ankyrin-G in rat hippocampal cornu ammonis 1 after pilocarpine induced status epilepticus. *Brain Res* 2009;1270:112–20.
24 Trudeau MM, Dalton JC, Day JW, Ranum LP, Meisler MH. Heterozygosity for a protein truncation mutation of sodium channel SCN8A in a patient with cerebellar atrophy, ataxia, and mental retardation. *J Med Genet* 2006;43:527–30.
25 Veeramah KR, O'Brien JE, Meisler MH, Cheng X, Dib-Hajj SD, Waxman SG, Talwar D, Girirajan S, Eichler EE, Restifo LL, Erickson RP, Hammer MF. De novo pathogenic SCN8A mutation identified by whole-genome sequencing of a family quartet affected by infantile epileptic encephalopathy and SUDEP. *Am J Hum Genet* 2012;90:502–10.
26 Carvill GL, Heavin SB, Yendle SC, McMahon JM, O'Roak BJ, Cook J, Khan A, Dorschner MO, Weaver M, Calvert S, Malone S, Wallace G, Stanley T, Bye AM, Bleasel A, Howell KB, Kivity S, Mackay MT, Rodriguez-Casero V, Webster R, Korczyn A, Afawi Z, Zelnick N, Lerman-Sagie T, Lev D, Moller RS, Gill D, Andrade DM, Freeman JL, Sadleir LG, Shendure J, Berkovic SF, Scheffer IE, Mefford HC. Targeted resequencing in epileptic encephalopathies identifies de novo mutations in CHD2 and SYNGAP1. *Nat Genet* 2013;45:825–30.
27 Epi4K Consortium, Epilepsy Phenome/Genome ProjectAllen AS, Berkovic SF, Cossette P, Delanty N, Dlugos D, Eichler EE, Epstein MP, Glauser T, Goldstein DB, Han Y, Heinzen EL, Hitomi Y, Howell KB, Johnson MR, Kuzniecky R, Lowenstein DH, Lu YF, Madou MR, Marson AG, Mefford HC, Esmaeeli Nieh S, O'Brien TJ, Ottman R, Petrovski S, Poduri A, Ruzzo EK, Scheffer IE, Sherr EH, Yuskaitis CJ, Abou-Khalil B, Alldredge BK, Bautista JF, Berkovic SF, Boro A, Cascino GD, Consalvo D, Crumrine P, Devinsky O, Dlugos D, Epstein MP, Fiol M, Fountain NB, French J, Friedman D, Geller EB, Glauser T, Glynn S, Haut SR, Hayward J, Helmers SL, Joshi S, Kanner A, Kirsch HE, Knowlton RC, Kossoff EH, Kuperman R, Kuzniecky R, Lowenstein DH, McGuire SM, Motika PV, Novotny EJ, Ottman R, Paolicchi JM, Parent JM, Park K, Poduri A, Scheffer IE, Shellhaas RA, Sherr EH, Shih JJ, Singh R, Sirven J, Smith MC, Sullivan J, Lin Thio L, Venkat A, Vining EP, Von Allmen GK, Weisenberg JL, Widdess-Walsh P, Winawer MR. De novo mutations in epileptic encephalopathies. *Nature* 2013;501:217–21.
28 Estacion M, O'Brien JE, Conravey A, Hammer MF, Waxman SG, Dib-Hajj SD, Meisler MH. A novel de novo mutation of SCN8A (Nav1.6) with enhanced channel activation in a child with epileptic encephalopathy. *Neurobiol Dis* 2014;69:117–23.
29 Vaher U, Noukas M, Nikopensius T, Kals M, Annilo T, Nelis M, Ounap K, Reimand T, Talvik I, Ilves P, Piirsoo A, Seppet E, Metspalu A, Talvik T. De Novo SCN8A mutation identified by whole-exome sequencing in a boy with neonatal epileptic encephalopathy, multiple congenital anomalies, and movement disorders. *J Child Neurol* 2014;29:NP202–6.
30 Ohba C, Kato M, Takahashi S, Lerman-Sagie T, Lev D, Terashima H, Kubota M, Kawawaki H, Matsufuji M, Kojima Y, Tateno A, Goldberg-Stern H, Straussberg R, Marom D, Leshinsky-Silver E, Nakashima M, Nishiyama K, Tsurusaki Y, Miyake N, Tanaka F, Matsumoto N, Saitsu H. Early onset epileptic encephalopathy caused by de novo SCN8A mutations. *Epilepsia* 2014;55:994–1000.
31 Larsen J, Carvill GL, Gardella E, Kluger G, Schmiedel G, Barisic N, Depienne C, Brilstra E, Mang Y, Nielsen JE, Kirkpatrick M, Goudie D, Goldman R, Jähn JA, Jepsen B, Gill D, Döcker M, Biskup S, McMahon JM, Koeleman B, Harris M, Braun K, de Kovel CG, Marini C, Specchio N, Djémié T, Weckhuysen S, Tommerup N, Troncoso M, Troncoso L, EuroEPINOMICS RES CRP, Bevot A, Wolff M, Hjalgrim H, Guerrini R, Scheffer IE, Mefford HC, Møller RS. The phenotypic spectrum of SCN8A encephalopathy. *Neurology* 2015;84:480–9.
32 de Kovel CG, Meisler MH, Brilstra EH, van Berkestijn FM, Slot RV, van Lieshout S, Nijman IJ, O'Brien JE, Hammer MF, Estacion M, Waxman SG, Dib-Hajj SD, Koeleman BP. Characterization of a de novo SCN8A mutation in a patient with epileptic encephalopathy. *Epilepsy Res* 2014;108:1511–18.
33 de Ligt J, Willemsen MH, van Bon BW, Kleefstra T, Yntema HG, Kroes T, Vulto-van Silfhout AT, Koolen DA, de Vries P, Gilissen C, del Rosario M, Hoischen A, Scheffer H, de Vries BB, Brunner HG, Veltman JA, Vissers LE. Diagnostic exome sequencing in persons with severe intellectual disability. *N Engl J Med* 2012;367:1921–9.
34 Vissers LE, de Ligt J, Gilissen C, Janssen I, Steehouwer M, de Vries P, van Lier B, Arts P, Wieskamp N, del Rosario M, van Bon BW, Hoischen A, de Vries BB, Brunner HG, Veltman JA. A de novo paradigm for mental retardation. *Nat Genet* 2010;42:1109–12.
35 Neveling K, Feenstra I, Gilissen C, Hoefsloot LH, Kamsteeg EJ, Mensenkamp AR, Rodenburg RJ, Yntema HG, Spruijt L, Vermeer S, Rinne T, van Gassen KL, Bodmer D, Lugtenberg D, de Reuver R, Buijsman W, Derks RC, Wieskamp N, van den Heuvel B, Ligtenberg MJ, Kremer H, Koolen DA, van de Warrenburg BP, Cremers FP, Marcelis CL, Smeitink JA, Wortmann SB, van Zelst-Stams WA, Veltman JA, Brunner HG, Scheffer H, Nelen MR. A post-hoc comparison of the utility of sanger sequencing and exome sequencing for the diagnosis of heterogeneous diseases. *Hum Mutat* 2013;34:1721–6.
36 Herzog RI, Liu C, Waxman SG, Cummins TR. Calmodulin binds to the C terminus of sodium channels Nav1.4 and Nav1.6 and differentially modulates their functional properties. *J Neurosci* 2003;23:8261–70.
37 Zhao Y, Yarov-Yarovoy V, Scheuer T, Catterall WA. A gating hinge in Na+ channels; a molecular switch for electrical signaling. *Neuron* 2004;41:859–65.
38 Brackenbury WJ, Calhoun JD, Chen C, Miyazaki H, Nukina N, Oyama F, Ranscht B, Isom LL. Functional reciprocity between Na+ channel Nav1.6 and beta1 subunits in the coordinated regulation of excitability and neurite outgrowth. *Proc Natl Acad Sci USA* 2010;107:2283–8.
39 Cestele S, Schiavon E, Rusconi R, Franceschetti S, Mantegazza M. Nonfunctional NaV1.1 familial hemiplegic migraine mutant transformed into gain of function by partial rescue of folding defects. *Proc Natl Acad Sci USA* 2013;110:17546–51.

40 Sharkey LM, Jones JM, Hedera P, Meisler MH. Evaluation of SCN8A as a candidate gene for autosomal dominant essential tremor. *Parkinsonism Relat Disord* 2009;15:321–3.
41 O'Brien JE, Sharkey LM, Vallianatos CN, Han C, Blossom JC, Yu T, Waxman SG, Dib-Hajj SD, Meisler MH. Interaction of voltage-gated sodium channel Nav1.6 (SCN8A) with microtubule-associated protein Map1b. *J Biol Chem* 2012;287:18459–66.
42 Catterall WA, Dib-Hajj S, Meisler MH, Pietrobon D. Inherited neuronal ion channelopathies: new windows on complex neurological diseases. *J Neurosci* 2008;28:11768–77.
43 Ceulemans BP, Claes LR, Lagae LG. Clinical correlations of mutations in the SCN1A gene: from febrile seizures to severe myoclonic epilepsy in infancy. *Pediatr Neurol* 2004;30:236–43.
44 Oliva M, Berkovic SF, Petrou S. Sodium channels and the neurobiology of epilepsy. *Epilepsia* 2012;53:1849–59.
45 Tai C, Abe Y, Westenbroek RE, Scheuer T, Catterall WA. Impaired excitability of somatostatin- and parvalbumin-expressing cortical interneurons in a mouse model of Dravet syndrome. *Proc Natl Acad Sci USA* 2014;111:E3139–48.
46 Kalume F, Westenbroek RE, Cheah CS, Yu FH, Oakley JC, Scheuer T, Catterall WA. Sudden unexpected death in a mouse model of Dravet syndrome. *J Clin Invest* 2013;123:1798–808.
47 Ogiwara I, Iwasato T, Miyamoto H, Iwata R, Yamagata T, Mazaki E, Yanagawa Y, Tamamaki N, Hensch TK, Itohara S, Yamakawa K. Nav1.1 haploinsufficiency in excitatory neurons ameliorates seizure-associated sudden death in a mouse model of Dravet syndrome. *Hum Mol Genet* 2013;22:4784–804.
48 Larkin MA, Blackshields G, Brown NP, Chenna R, McGettigan PA, McWilliam H, Valentin F, Wallace IM, Wilm A, Lopez R, Thompson JD, Gibson TJ, Higgins DG. Clustal W and Clustal X version 2.0. *Bioinformatics* 2007;23:2947–8.

Clinical exome sequencing

Patients with unexplained sporadic ID are subjected to 'trio'-exome sequencing to detect potentially pathogenic *de novo* (in dominant conditions) or inherited (in recessive conditions) mutations[1]. For familial ID or other inherited disorders, such as movement disorders, singleton sequencing of the patient is the usual approach. Clinical exome sequencing (both trio and singleton) is analyzed in a two-tiered approach. First, exome sequencing data are pre-filtered for mutations in the respective ID or movement disorder gene panels before manual inspection[2]. Second, if no causative mutations were identified in the first step and patients (or legal guardians) consented, the entire dataset was filtered for likely-causative mutations (which may or may not be in OMIM genes). Informed consent for clinical exome sequencing is obtained by clinical geneticists in accordance with local regulations and this procedure was approved by the medical ethics committee of the Radboud university medical center.

Exome sequencing was performed essentially as previously described [2]. Briefly, genomic DNA was fragmented and exome fragments were captured using the SureSelect^{XT} Human All Exon 50Mb Kit (Agilent). The fragments were amplified by emulsion PCR and subjected to sequencing on a SoliD 5500XL^{TM} (Life Technologies) or a HiSeq2000^{TM} machine (Illumina). Data from the 5500XL machine were analysed using Bioscope^{TM} (version 2.0, Life Technologies) and the Hiseq2000 data were analysed with BWA (read alignment,[3]) and GATK (variant calling,[4]) software packages. Variants were annotated using an in-house developed pipeline. Prioritization of variants was done by an in-house designed 'variant interface' and manual curation. Potentially causative variants were confirmed by Sanger sequencing.

1 de Ligt J, Willemsen MH, van Bon BW, Kleefstra T, Yntema HG, Kroes T, Vulto-van Silfhout AT, Koolen DA, de Vries P, Gilissen C, del Rosario M, Hoischen A, Scheffer H, de Vries BB, Brunner HG, Veltman JA, Vissers LE. Diagnostic exome sequencing in persons with severe intellectual disability. *N Engl J Med* 2012;**367**(20):1921-9.

2 Neveling K, Feenstra I, Gilissen C, Hoefsloot LH, Kamsteeg EJ, Mensenkamp AR, Rodenburg RJ, Yntema HG, Spruijt L, Vermeer S, Rinne T, van Gassen KL, Bodmer D, Lugtenberg D, de Reuver R, Buijsman W, Derks RC, Wieskamp N, van den Heuvel B, Ligtenberg MJ, Kremer H, Koolen DA, van de Warrenburg BP, Cremers FP, Marcelis CL, Smeitink JA, Wortmann SB, van Zelst-Stams WA, Veltman JA, Brunner HG, Scheffer H, Nelen MR. A post-hoc comparison of the utility of sanger sequencing and exome sequencing for the diagnosis of heterogeneous diseases. *Hum Mutat* 2013;**34**(12):1721-6.

3 Li H, Durbin R. Fast and accurate long-read alignment with Burrows-Wheeler transform. *Bioinformatics* 2010;**26**(5):589-95.

4 McKenna A, Hanna M, Banks E, Sivachenko A, Cibulskis K, Kernytsky A, Garimella K, Altshuler D, Gabriel S, Daly M, DePristo MA. The Genome Analysis Toolkit: a MapReduce framework for analyzing next-generation DNA sequencing data. *Genome Res* 2010;**20**(9):1297-303.

Patient 1 was born after an uneventful pregnancy and delivery. Her birth weight was 3,050 grams (40th percentile). She was the second child of healthy non-consanguineous parents. Hypertonia was noticed immediately after birth. At six weeks of age, she was diagnosed with non-febrile generalized seizures. The seizures were frequent and intractable and included multiple seizure types such as infantile spasms, clonic seizures with cyanosis, myoclonic complex partial and absences seizures. Her development was severely delayed. At the age of 11 months her developmental age was 1 month. She had a severe dysregulation of muscle tone. Chromosomal analysis, including genome-wide array analysis, showed no abnormalities. DNA diagnostics for the *POLG* gene (mitochondrial DNA depletion syndrome), blood chemistries and a metabolic screen in urine revealed no abnormalities. At the age of 3 years, DNA sequencing of *FOXG1*, *ARX* and *CDKL5* was performed because of persistent seizures and severe developmental delay. Results were normal. After the age of 3 years, treatment with multiple antiepileptic agents (phenobarbital, phenytoin, levetiracetam , clobazam and zonisamide) led to seizure control.

At the age of 7 years she was wheelchair dependent, and unable to sit independently or speak. She was fed by a percutaneous endoscopic gastrostomic tube. She had to be catheterized intermittently because of a neurogenic bladder due to a tethered cord. Upon physical examination she had a height of 121 cm (>50th centile) and a head circumference of 51.5 cm (>50th centile). Minor facial dysmorphisms included synophris, broad nasal tip and upslanted palpebral fissures. Hirsutism was probably due to treatment with the anti-epileptic drug phenytoin. A right convex thoracic scoliosis and tapering fingers were observed. MRI demonstrated progressive cerebral atrophy (Supplementary Figure 1).

Patient 2 was born after uneventful pregnancy and delivery. His birth weight was normal (3,000 grams, 16th percentile). At six months, hypertonia and an abnormal head posture were observed. Onset of seizures at 18 months was said to follow an episode of meningitis. He

presented with a severe global developmental delay. At the age of six years, he learned to walk independently and spoke his first words. As an adult, his developmental level was comparable to a child of 4-5 years. Seizures were generally well controlled by treatment with carbamazepine, although he had absence-like episodes and occasional tonic-clonic seizures. After the age of 29 years, he had a gradual decline in motor function and lost the ability to walk independently, to climb stairs and to cycle. He also developed balance problems and ataxia, leading to recurrent falls and swallowing difficulties. In parallel there was a decline in cognitive functioning, albeit less pronounced. Upon the last examination at the age of 31 years he had a head circumference of 55,2 cm (5^{th}-10^{th} percentile). He showed a gaze-evoked nystagmus, jerky pursuit, and a slight limitation in upward gaze. In addition he had a spastic tetraparesis with a broad based, spastic gait. Lower limb reflexes were brisk with equivocal plantar reflexes. There were no facial dysmorphisms. An MRI brain scan showed cerebellar atrophy (Supplementary Figure 2). Genome-wide chromosomal analysis by 250k SNP array analysis and metabolic tests, including a screen of blood and urine and lysosomal enzyme activity measurements in fibroblasts, revealed no abnormalities.

Patient 3 was born after an uneventful pregnancy and delivery. He had a normal birth weight of 2,880 grams (25^{th} percentile). He was the first child in his family and has two healthy younger brothers. His parents reported an early delay in development, with independent walking after the age of 18 months. Speech development was delayed and he cannot read or write. Eye contact was poor. He had to attend a special school. Formal intelligence tests showed an intelligence quotient of 50. At the age of 15 years he was diagnosed with an autism spectrum disorder (ASD) and at 17 years he was moved to a sheltered home because of problematic behaviours including aggressive outbursts and self-mutilation. He had an anxious and insecure personality and was diagnosed with mild hypothyroidism. He was operated on at six weeks for unilateral inguinal hernia, and at 18 months for an umbilical hernia, but was

otherwise in good medical condition. He had no seizures and a normal electroencephalogram at 4 years of age. A cerebral CT-scan showed atypical anomalies including atrophy of the frontal lobe and paramedian regions. At the age of 31 years his height was 169 cm (2^{nd} percentile), with weight of 78 kg (85^{th} percentile) and head circumference of 55.8 cm (10^{th} percentile). Facial dysmorphisms included a high forehead, full eyelids and ptosis, down turned corners of the mouth and a high and narrow palate. We also observed a sandal gap, flat feet, clinodactyly of both second fingers and a mild pectus excavatum. Genome-wide chromosomal analysis (karyotype and SNP-array), DNA diagnostics for Fragile X syndrome, and metabolic tests in blood and urine revealed no abnormalities. The patient was included in family-based whole-exome sequencing studies.

SUPPLEMENTARY FIGURE LEGENDS

Figure S1 Magnetic resonance imaging of patient 1. **MR imaging performed at the age of 3 months (A) and 3 years and 3 months (B). Both are T2-weighted transversal images. Note the progressive global cerebral atrophy.**

Figure S2 Magnetic resonance imaging of patient 2. MR imaging performed the age of 31 yr. The scan (T2 weighted; sagittal slice) demonstrates marked atrophy of the cerebellum. The scan is of suboptimal quality due to movement of the patient.

Figure S3 Protein expression of wildtype and mutant $Na_V1.6$ transfected in HEK293 cells. Western blotting of cell lysates expressing $Na_V1.6$ mutants shows similar expression of wt and G1451S-encoding channel constructs. The migration of expressed proteins, with apparent molecular weight of 250 kDa (top), corresponds to previous observations of mutant and wildtype protein [32]. Reprobing for α-tubulin indicates equal loading of cell lysates (bottom).

A

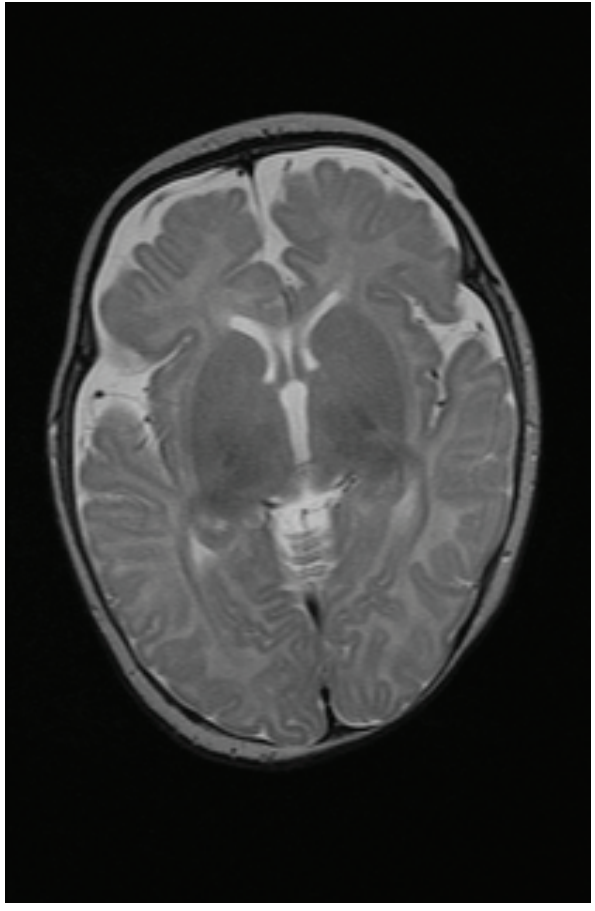

B

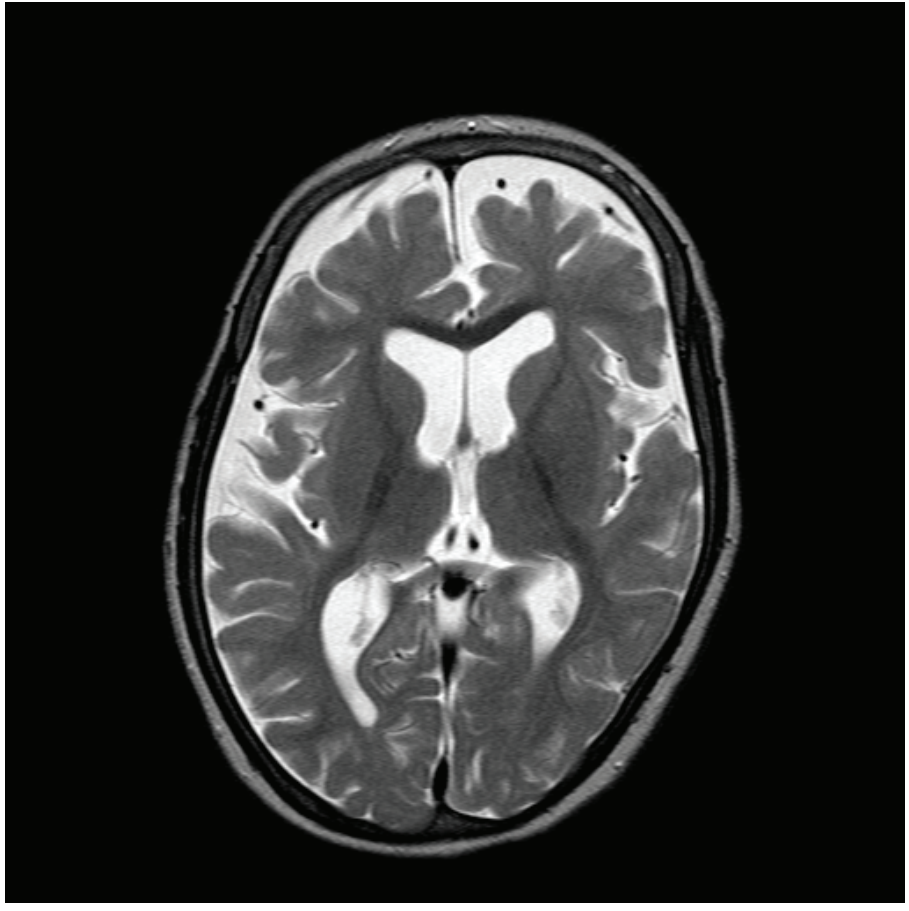

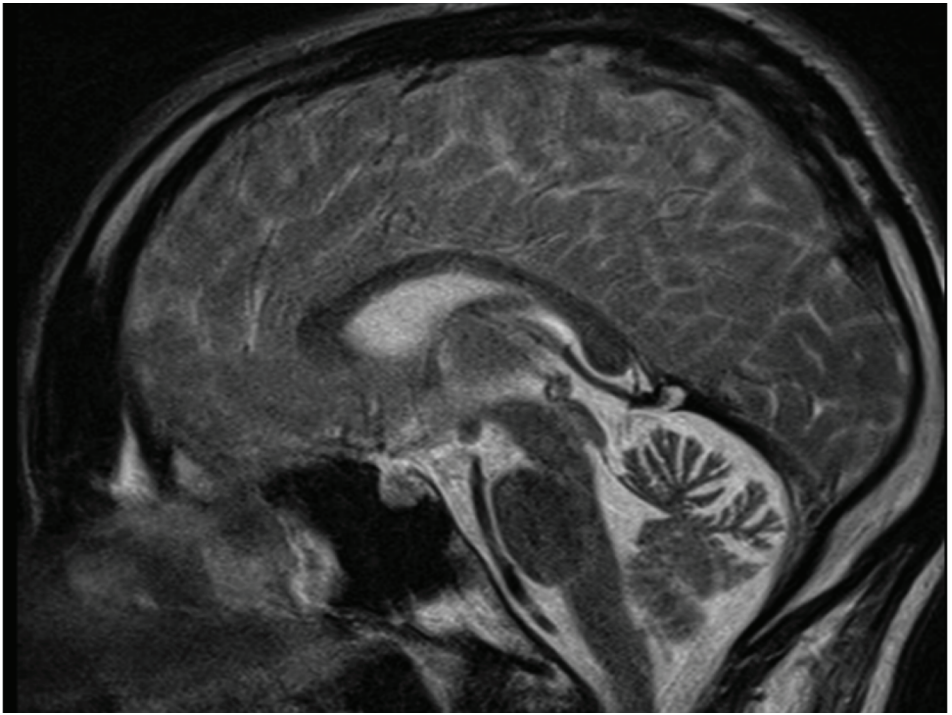

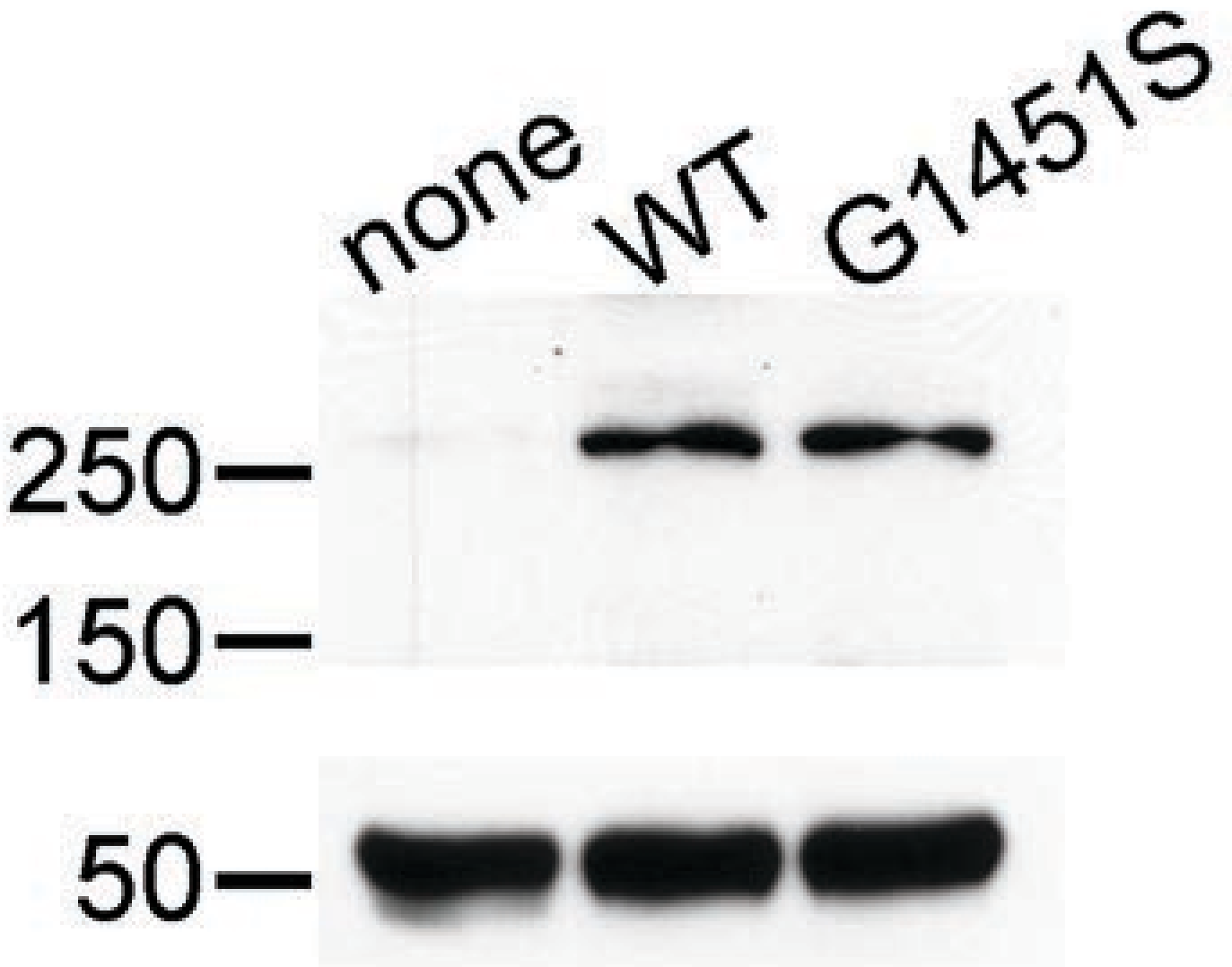
none
WT
G1451S
250
150
50